

Research Article

Theme: Recent Trends in the Development of Chitosan-Based Drug Delivery Systems
Guest Editors: Claudio Salomon, Francisco Goycoolea, and Bruno Moerschbacher

Albendazole Microcrystal Formulations Based on Chitosan and Cellulose Derivatives: Physicochemical Characterization and *In Vitro* Parasiticidal Activity in *Trichinella spiralis* Adult Worms

Josefina Priotti,¹ Ana V. Codina,² Darío Leonardi,^{1,3} María D. Vasconi,^{2,4}
Lucila I. Hinrichsen,^{2,5,7} and María C. Lamas^{1,3,6,7}

Received 19 August 2016; accepted 19 October 2016

Abstract. The oral route has notable advantages to administering dosage forms. One of the most important questions to solve is the poor solubility of most drugs which produces low bioavailability and delivery problems, a major challenge for the pharmaceutical industry. Albendazole is a benzimidazole carbamate extensively used in oral chemotherapy against intestinal parasites, due to its extended spectrum activity and low cost. Nevertheless, the main disadvantage is the poor bioavailability due to its very low solubility in water. The main objective of this study was to prepare microcrystal formulations by the bottom-up technology to increase albendazole dissolution rate, in order to enhance its antiparasitic activity. Thus, 20 novel microstructures based on chitosan, cellulose derivatives, and poloxamer as a surfactant were produced and characterized by their physicochemical properties and *in vitro* biological activity. To determine the significance of type and concentration of polymer, and presence or absence of surfactant in the crystals, the variables area under the curve, albendazole microcrystal solubility, and drug released (%) at 30 min were analyzed with a three-way ANOVA. This analysis indicated that the microcrystals made with hydroxyethylcellulose or chitosan appear to be the best options to optimize oral absorption of the active pharmaceutical ingredient. The *in vitro* evaluation of anthelmintic activity on adult forms of *Trichinella spiralis* identified system S10A as the most effective, of choice for testing therapeutic efficacy *in vivo*.

KEY WORDS: albendazole; bottom-up microcrystal; chitosan; *in vitro* antiparasitic assay.

INTRODUCTION

Oral administration of dosage forms offers significant advantages over other routes. It is a straightforward and

comfortable route, providing many different options to control drug release and patient compliance during a chemotherapeutic treatment. However, in oral dosage forms, it is a well-known fact that drug solubility and dissolution rate have a critical role in its absorption (1). Therefore, the most important issue to be solved, and a major challenge for the pharmaceutical industry, is the poor water solubility of drugs, which results in low bioavailability and delivery problems (2,3).

Several strategies have been used to improve the solubility and the dissolution rate of active pharmaceutical ingredients (APIs). Developing novel nano- and microplatforms have been one of the most useful alternatives (4–7). During the '90 Müller *et al.*, working on the development of nano- and microsuspensions and nano- and microcrystals drew attention to the influence of particle size on the rate of dissolution and absorption of a drug. That appeared to be mainly true for compounds of class II and IV (8–10). There are numerous strategies for making nano- and microsized drug particles, and those are broadly classified

¹ IQUIR-CONICET, Suipacha 570, 2000, Rosario, Argentina.

² Instituto de Genética Experimental, Facultad de Ciencias Médicas, Universidad Nacional de Rosario, Santa Fe 3100, S2000KTR, Rosario, Argentina.

³ Departamento de Farmacia, Facultad de Ciencias Bioquímicas y Farmacéuticas, Universidad Nacional de Rosario, Suipacha 570, 2000, Rosario, Argentina.

⁴ Área Parasitología, Facultad de Ciencias Bioquímicas y Farmacéuticas, Universidad Nacional de Rosario, Suipacha 570, 2000, Rosario, Argentina.

⁵ CIC-UNR, Universidad Nacional de Rosario, Maipú 1065, 2000, Rosario, Argentina.

⁶ Facultad de Ciencias Bioquímicas y Farmacéuticas, Universidad Nacional de Rosario, Suipacha 531, 2000, Rosario, Argentina.

⁷ To whom correspondence should be addressed. (e-mail: lhinrich@unr.edu.ar; mlamas@fbiof.unr.edu.ar)

into four categories as bottom-up, top-down, combination approaches, and chemical synthesis (11–13). The applicability of these techniques differs among molecules and depends on the physicochemical characteristics of each molecule (14). The bottom-up approach relies on controlled precipitation/crystallization. The process involves dissolving the drug in a solvent and precipitating it in a controlled manner by the addition of an antisolvent (15,16). The procedure requires the use of polymers and surfactants to stabilize and decrease the particle size in addition to modifying the solid structure of the API (16–18). The chosen natural biopolymers are chitosan (CH) and cellulose derivatives.

CH is a natural, biodegradable polymer with a considerable potential for pharmaceutical applications as an excipient, due to its biocompatibility, nontoxicity, and mucoadhesiveness. This material is especially interesting for the pharmaceutical industry not only because it is made from a productive renewable resource but because it is effective in many biological applications and has antimicrobial activity, low immunogenicity, and ecological safety (19–22).

There are many semisynthetic derivatives of cellulose currently used in the pharmaceutical and cosmetic industries. These polymers are broadly employed in the formulation of dosage forms and healthcare products (19,20,23–29).

Albendazole (ABZ) is the most extensively selected API for oral treatment of trichinellosis, a parasitic disease caused by the helminth *Trichinella* spp. ABZ is a broad spectrum anthelmintic showing larvicide, oxicide, and vermicide activity (30). Its efficacy in the treatment of trichinellosis is strictly related to the time of administration; in fact, it is more effective in the early stages of infection, when the worms are still present in the intestinal mucosa or newborn larvae are migrating from intestinal vessels to muscles. ABZ, as other

benzimidazoles, is classified as class II by the Biopharmaceutics Classification System, since it has an extremely poor aqueous solubility which limits oral absorption (31).

The aim of this work was to produce ABZ microcrystal formulations by the bottom-up technology and its full physicochemical characterization and the *in vitro* evaluation of the anthelmintic activity.

MATERIALS AND METHODS

Materials

ABZ, hydroxypropyl methylcellulose (HPMC), viscosity 4680 cPs (2%, 20°C), hydroxyethyl cellulose (HEC), viscosity 100 cPs (1%, 20°C), methylcellulose (MC), viscosity 4000 cPs (1%, 20°C), carboxymethylcellulose (CMC), sodium viscosity 4000 cPs (1%, 20°C), and chitosan (CH) (M_w 310–375 kDa >75% deacetylated) were obtained from Sigma-Aldrich Chemie GmbH (Steinheim, Germany). Poloxamer 338 (P338), Pluronic® F 108NF, was purchased from BASF (NJ, USA), RPMI 1640 from Sigma-Aldrich Chemie GmbH (Steinheim, Germany), and fetal bovine serum and gentamicin from Klonal (Argentina). All other chemicals were of analytical grade.

Microcrystal Formulations

ABZ (400 mg) was dissolved in glacial acetic acid (4 mL) and ethanol (6 mL). The resulting solution was dropped over 100 mL of the polymeric solution prepared as follows: CH was dissolved in 1% *v/v* acetic acid solution and cellulose derivatives and the surfactant P338 were dissolved in water (Table I). The

Table I. Microcrystal Formulation, Composition, Solubility, AUC, Q_{30} , and Yield

System	Polymer	Polymer concentration (% <i>w/v</i>)	Surfactant P338	Yield (%)	AUC	Q_{30} (%)	Solubility (mg/mL)
ABZ	–	–	–	–	1802	2.87	0.27
S1A	HPMC	0.5	No	23.71	16,780	28.52	1.18
S1B	HPMC	0.5	Yes	46.12	11,880	19.47	1.38
S2A	HPMC	0.1	No	26.82	25,330	66.82	1.07
S2B	HPMC	0.1	Yes	84.76	22,950	64.77	0.98
S3A	HEC	0.5	No	39.14	29,160	92.79	1.03
S3B	HEC	0.5	Yes	50.29	26,820	75.86	0.95
S4A	HEC	0.1	No	81.08	30,110	96.84	0.79
S4B	HEC	0.1	Yes	83.19	29,200	80.29	0.70
S5A	CMC	0.5	No	33.22	6694	9.66	0.68
S5B	CMC	0.5	Yes	57.83	19,230	28.82	0.71
S6A	CMC	0.1	No	23.99	6915	12.91	0.67
S6B	CMC	0.1	Yes	86.04	23,580	58.71	0.86
S7A	MC	0.5	No	46.67	4059	4.94	0.66
S7B	MC	0.5	Yes	47.79	16,680	25.41	0.82
S8A	MC	0.1	No	27.04	6160	7.58	0.57
S8B	MC	0.1	Yes	97.12	7831	10.55	0.80
S9A	CH	0.5	No	89.72	26,360	98.60	0.34
S9B	CH	0.5	Yes	50.98	25,060	53.34	0.56
S10A	CH	0.1	No	59.79	21,280	48.54	0.38
S10B	CH	0.1	Yes	47.39	25,860	85.65	0.73

AUC area under the curve, ABZ albendazole, HPMC hydroxypropyl methylcellulose, CMC carboxymethylcellulose, MC methylcellulose, CH chitosan, HEC hydroxyethyl cellulose

Albendazole Microcrystal Formulations

ABZ solution and the polymeric/surfactant solution were combined under magnetic stirring at 1000 rpm. After 10 min, the suspension was dried using a spray-drying procedure, in a Mini Spray Dryer Büchi B-290 (Flawil, Switzerland) under the following conditions: inlet temperature 130°C, outlet temperature 70°C, air flow 38 m³/h, feed rate 5 mL/min, and aspirator set 100%.

Solubility Studies

ABZ solubility of the microstructured systems was analyzed in an orbital shaker (Boeco, Germany), at room temperature (25°C). For each formulation, an excess amount of microcrystal powder was placed in a vial containing 0.1 N HCl and was stirred at 150 rpm for 72 h. The resulting suspension was filtered, and ABZ concentration was determined by UV spectroscopy at 291 nm with an S-26 UV-Vis spectrophotometer Boeco (Hamburg, Germany).

Differential Scanning Calorimetry

Differential scanning calorimetry (DSC) was performed on a Shimadzu TA-60 (Kyoto, Japan) calorimeter, using 5 mg samples in crimped aluminum pans. The instrument was calibrated with indium and zinc as standards. Nitrogen was used as a purge gas and an empty aluminum pan as a reference. Each sample was scanned at a rate of 5°C/min from 25 to 350°C, under N₂ atmosphere (flow rate 30 mL/min).

X-Ray Diffraction

Data collection was carried out in transmission mode on an automated X'Pert Phillips MPD diffractometer (Eindhoven, The Netherlands).

X-ray diffraction (XRD) patterns were recorded using CuK α radiation ($\lambda = 1.540562 \text{ \AA}$), a voltage of 40 kV, 20 mA current, and steps of 0.02° on the interval $2\theta = 10^\circ\text{--}40^\circ$. Low peak broadening and background were ensured by using parallel beam geometry with the help of x-ray lens and a graphite monochromator placed before the detector window.

Data acquisition and evaluation were performed with the Stoe Visual-Xpov package, version 2.75 (Germany).

Dissolution Studies

Dissolution assays were conducted in a USP Standard Dissolution Apparatus Hanson Research SR8 Plus (Chatsworth, USA), equipped with a rotational paddle (50 rpm), following the US Pharmacopeia conditions for ABZ tablets: dissolution medium (900 mL of 0.1 N HCl) at 37°C. Microcrystal formulations containing ABZ (100 mg) were introduced into the flasks. Three samples were taken at 10, 20, 30, 45, 60, 90, 120, 180, 240, and 300 min (32).

They were sampled in triplicate at 10, 20, 30, 45, 60, 90, 120, 180, 240, and 300 min (32), using a filter, to determine the amount of ABZ released. An equal volume of the dissolution medium was added after each sample extraction to maintain a constant volume. The polymers did not interfere with the assay at the working wavelength (291 nm). Dissolution efficiency (DE) of the microcrystal dosage

forms (33) is defined as the area under a dissolution curve between specified time points, was calculated using the following equation:

$$\text{Dissolution efficiency \% (DE)} = \frac{\int_0^t y \cdot dt}{y_{100} \cdot t} \times 100 \quad (1)$$

where y is the percentage of dissolved product at time t .

Microcrystals Yield

The yield (Y) was calculated as the ratio between the experimental weight of the product and the sum of the weights of all the components:

$$Y(\%) = 100 \times [W_{\text{product}} / (W_{\text{ABZ}} + W_{\text{polymer}} + W_{\text{surfactant}})] \quad (2)$$

where W_{product} is the weight of the obtained microcrystals, and W_{ABZ} , W_{polymer} , and $W_{\text{surfactant}}$ are the weights of ABZ, polymers, and the surfactant, respectively.

Determination of ABZ Content in the Microcrystal Formulations

The entrapment efficiency (EE) is defined as the percentage of the final drug content, relative to the initial amount of loaded drug. For the EE determination, microcrystals were dissolved in 0.1 N HCl for 24 h. The amount of loaded drug was measured spectrophotometrically at 291 nm with a Boeco S-26 spectrophotometer (Hamburg, Germany), according to the following:

$$\text{EE}(\%) = 100 \times (W_{\text{ABZ}} / W_{\text{tABZ}}) \quad (3)$$

where W_{ABZ} is the actual ABZ content, and W_{tABZ} is theoretical ABZ content in the microcrystals.

Morphology Analysis and Size Determination by Scanning Electron Microscopy

Particle size and morphology were determined through images by scanning electron microscopy (SEM) using a Leitz AMR 1600 T (Amray, Bedford, MA, USA), with an acceleration potential of 20 kV. Samples were previously sputter-coated with a gold layer to make them conductive.

Moreover, to determine an indirect estimation of the microcrystals' particle size, SEM images were analyzed using the Image-pro Plus (IPP) software v. 6.0. This procedure involves the determination of the Feret's diameter of a particle which is a commonly used measure in shape analysis. Feret's diameter is the distance between the two furthest points of the shape measured in a given direction. About 200 microcrystal Feret's diameters were considered in each particle size distribution calculation (34,35).

In Vitro Anthelmintic Activity of ABZ-Microcrystals

Preparation of *Trichinella spiralis* Female Worms

CBI mice given an oral dose of 10 L1 *T. spiralis* larvae per gram body weight were sacrificed in the intestinal phase of the infection, on day 6 post-infection, as already described (36). Briefly, animals were euthanized, and the small intestine was removed, cut into several pieces of roughly equal length and placed on Petri dishes with 8–12 mL of 0.85% w/v NaCl plus 250 µg/mL gentamicin (incubation medium). Each piece was then opened lengthwise using a small iris scissors, grasped with forceps, agitated gently in the medium, and incubated for 4 h at 37°C in 5% CO₂. After incubation, the pieces of intestine were rinsed with the medium onto the Petri dish and discarded. All the content of the Petri dishes was transferred to centrifuge tubes and centrifuged at low speed. The parasite pellet was re-suspended in approximately 2–3 mL RPMI 1640 medium supplemented with gentamicin and fetal bovine serum (250 µg/mL and 10% v/v, respectively) and placed in a sterile plate, to identify and separate the female worms for the assay. Animals were treated in accordance with the institutional regulations which comply with the guidelines issued by the Institute for Laboratory Animal Resources, National Research Council, USA (36). All experiments involving animals were performed with prior approval from the Bioethics Committee of the Facultad de Ciencias Médicas, Universidad Nacional de Rosario, Argentina, permit number C.S. 1115/2014.

Preparation of the Antiparasitic Solutions

ABZ and ABZ microstructured systems stock solutions were prepared in dimethyl sulfoxide (DMSO) at a concentration of 10 mg/mL. Each working solution was made with RPMI 1640 medium containing gentamicin (250 µg/mL) and DMSO (up to a maximum of 2%) to obtain a concentration of 500 µg/mL of ABZ. They were stirred at room temperature for 24 h and then filtered through sterile cellulose acetate filters 0.2 µm pore (Minisart®, Sartorius Stedim Biotech, USA).

In Vitro Assay

The whole procedure was done under sterile conditions. *T. spiralis* female worms obtained as described above were incubated overnight in RPMI 1640 supplemented with gentamicin (250 µg/mL) and fetal bovine serum (10% v/v) at 37°C, in a 5% CO₂ atmosphere, before being used. For the assay, females were placed in 24-well cell culture plates (10 to 12 per well) which contained the antiparasitic ABZ-microcrystal solutions to be tested supplemented with 10% fetal bovine serum. The ABZ solution was used as a positive control and the culture medium with the solvent employed as a negative control. The worms were incubated in a humid 5% CO₂ atmosphere at 37°C during 48 h and were observed with an inverted microscope at 2, 4, 7, 24, 29, and 48 h. At each time, female viability was estimated analyzing their motility and morphology and were counted as “live” or “dead”; the amount and motility of newborn larvae were also examined. The effect of the various antiparasitic solutions on median worm survival was calculated by means of a survival curve.

Experiments were carried out in duplicate, and data were corrected with the negative control.

Statistical Analysis

A three-way ANOVA analysis (SigmaPlot 12.0 software) was done to determine how solubility of ABZ in microcrystal systems was affected by the different factors. The factors considered were type of polymer (HPMC, HEC, CMC, MC, or CH), polymer concentration in aqueous solution (0.1 and 0.5% w/v), and presence or absence of surfactant (P338). The variables analyzed were area under the curve (AUC), ABZ microcrystal solubility, and percentage of drug released at 30 min of the dissolution assay (Q_{30}). AUCs were estimated in each of the dissolution plots using GraphPad Prism software (GraphPad Prism®; GraphPad Software Inc., San Diego, CA, USA).

Survival curves were calculated with the product limit method of Kaplan and Meier, using GraphPad Prism software. Comparison of the survival curves was done with the log-rank test.

A *P* value < 0.05 was considered significant.

RESULTS

Crystal Characterization

To determine the significance of type and concentration of polymer, and presence or absence of surfactant in the crystals, the responses AUC, ABZ microcrystal solubility, and Q_{30} values were analyzed with a three-way ANOVA. The interaction was not significant, and the effect of each factor on AUC, ABZ solubility, and Q_{30} was studied separately.

AUC was significantly different for each type of polymer ($P = 0.005$). Depending on the polymer used, AUC decreased in the following order: HEC > CH > HPMC > CMC > MC (Table I).

Neither polymer concentration nor presence or absence of the surfactant P338 had a significant influence over AUC ($P = 0.331$, $P = 0.072$, respectively) (Table I).

Figure 1a shows the influence of HPMC on the behavior of the microcrystal drug release. The addition of the surfactant modified the release rate, which is also noticeably determined by the polymer concentration: the lower the concentration, the faster the release rate. CMC and MC did not improve drug release rate (Fig. 1c, d). Figure 1 also shows clearly that the best results were obtained employing HEC (B) and CH (E) as stabilizing biopolymers, since more than 70% of the drug was released after 60 min.

Moreover, systems S4A y S10A achieved 99% EE. These results clearly show that the manufacturing process of the microcrystal formulations did not affect the drug concentration in the final product. It is worth mentioning that the apparent solubility assay data did not correspond with the obtained results by the dissolution studies, since solubility is not a valid physicochemical parameter to demonstrate the suitability of these microcrystal formulations to design oral dosage forms.

Furthermore, after carefully analyzing Fig. 2, higher yield values were obtained for microcrystals prepared with lower polymer concentration and the presence of the P338. Otherwise, CH and HEC microcrystals presented higher yield values at lower concentration of the polymers without surfactant.

SEM, Particle Size, DRX, and DSC Studies

SEM micrographs confirmed the crystalline structures, showing sharp and irregular shapes. Particle size was calculated employing the IPP software v. 6.0 (Fig. 3).

Albendazole Microcrystal Formulations

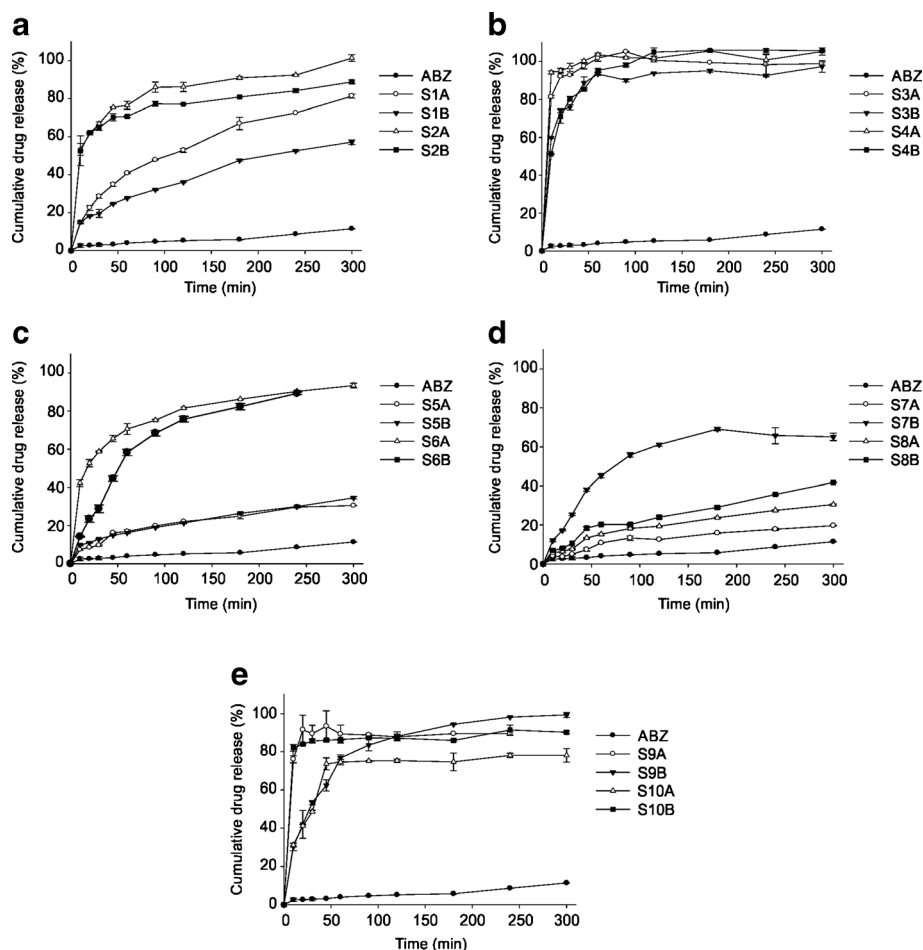


Fig. 1. Dissolution profiles of microcrystal systems and ABZ pure drug (0.1 N HCl medium, 37°C). **a** HPMC systems. **b** HEC systems. **c** CMC systems. **d** MC systems. **e** CH systems. ($n = 3 \pm SD$)

HPMC, CMC, and MC systems prepared employing higher polymer concentration exhibited bigger sizes than the obtained employing lower concentration. The presence of P338 produced also bigger particle size for HEC and CH systems.

The mean diameters of the S4A and S10A formulations were less than 4 μm (Fig. 4).

DSC thermograms of ABZ, S4A, and S10A are shown in Fig. 5a. The characteristic sharp melting peak of ABZ is

observed at 196.84°C. The intensity of the drug endothermic peak was also exhibited in the systems.

Figure 5b shows the XRD spectra of ABZ, and the systems S4A and S10A. ABZ presented intense and characteristic peaks at 2θ 11.51; 17.85; 22.09 y 24.54. The same peaks were observed in the microcrystal systems, confirming no changes in the drug solid structure after the manufacturing procedure.

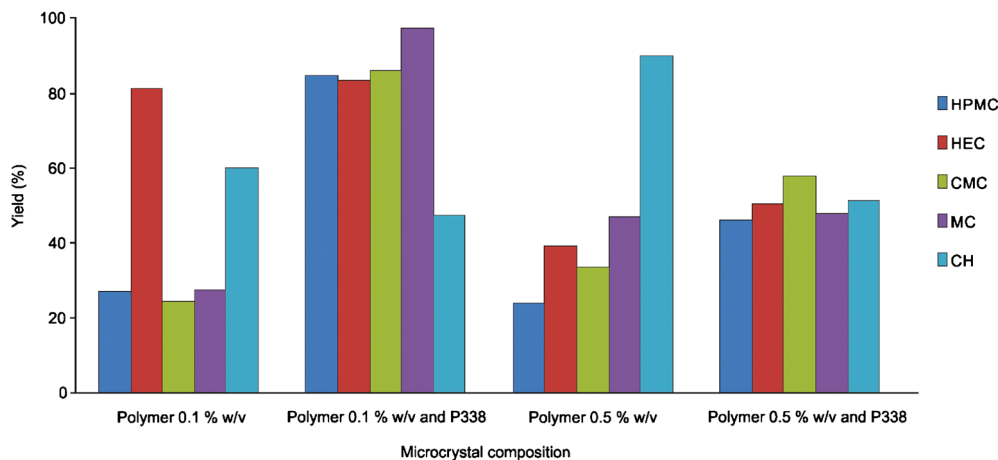


Fig. 2. Yield values (%) of microcrystal systems

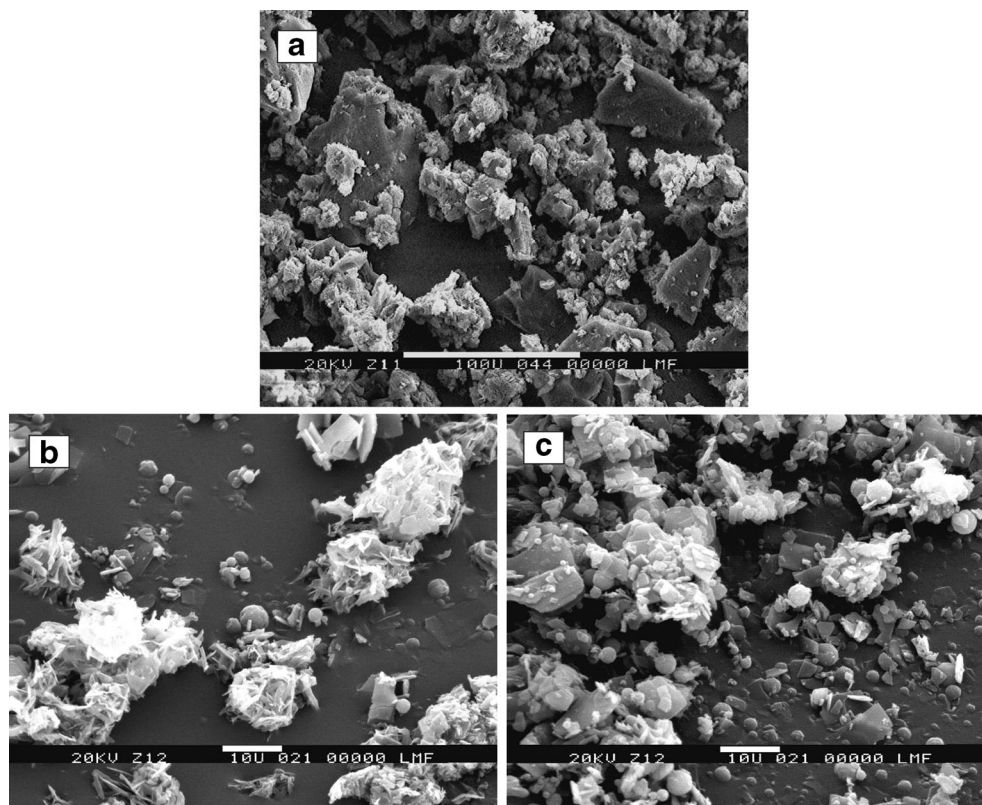


Fig. 3. SEM images. a ABZ ($\times 500$). b S10A ($\times 2000$). c S4A ($\times 2000$)

In Vitro Assay

The effect of the different microcrystal formulations on the *in vitro* ability of ABZ to kill adult *T. spiralis* worms was assessed by the survival curves of the parasite cultured for 48 h in medium RPMI 1640 containing the ABZ formulations (Fig. 6; Table II). Most formulations significantly improved ABZ parasiticidal activity ($P < 0.01$). Only S1A, S2B, S3B, S5A, and S6B showed a behavior similar to the pure drug with median survivals over 24 h and a high proportion of live worms at the end of the experiment.

Polymer concentration did not change, in general, the anthelmintic activity of the formulation. In a few cases (four of the 20 systems studied), the effect was significant but

random; different responses were observed depending on the polymer used. Systems based on HPMC, HEC, or CH were significantly more active at lower concentrations while the system containing HPMC and P338 improved its activity when the polymer concentration was increased.

Similar results were observed when the surfactant was added to the formulation. The microcrystal formulation with HPMC was the only one showing more activity with the addition of P338.

Figure 7 displays the survival curves of female worms cultured in contact with ABZ or ABZ microcrystal solutions. These microcrystal solutions were selected from each polymer group because they exhibited the best parasiticidal activity of the group. All the microcrystal solutions had a significantly better activity than the ABZ solution ($P < 0.01$), and S10A was considerably more efficient than the others ($P < 0.01$).

The effect of the formulations on the newborn larvae released by *T. spiralis* females exposed to the antiparasitic solutions was also examined. The mobility of the newborn larvae was affected to varying degrees by the formulations, showing complete loss of movement after 2 h and up to the end of the experiment, in culture media containing S4A, S5B, and S10A. The media containing the other systems had both mobile and immobile larvae in the studied period.

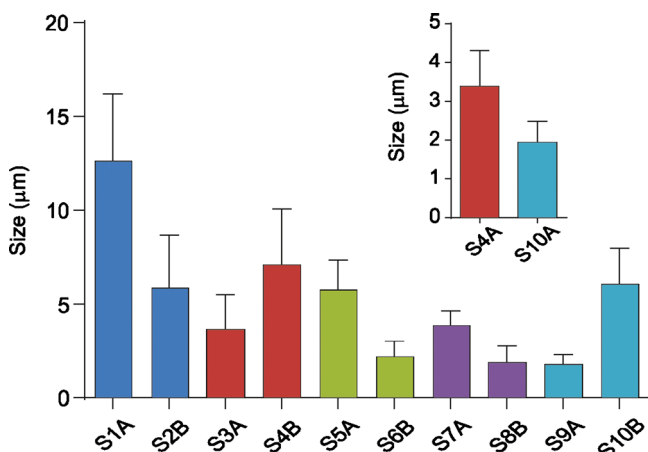


Fig. 4. Size of the microcrystals (bars represent standard deviation)

DISCUSSION

Twenty novel microstructures have been prepared and their physicochemical properties and *in vitro* biological activity were characterized.

It is well-known that the smaller the particle size, the larger the surface area and the faster the dissolution rate of

Albendazole Microcrystal Formulations

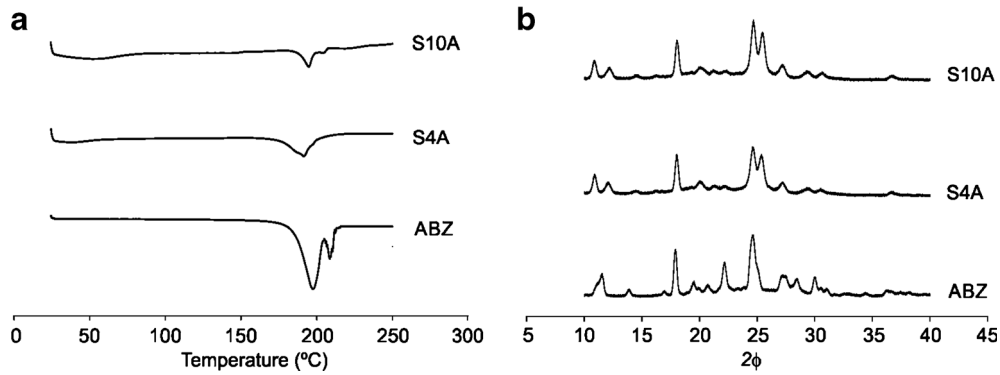


Fig. 5. a DSC curves: ABZ, S4A, and S10A. b XRD patterns: ABZ, S4A, and S10A

drug particles. This point could be explained according to the modified Noyes-Whitney equation:

$$dC/dt = AD(C_s - C)/h \quad (4)$$

where C_s the solubility of the drug, A the effective surface area, h the thickness of the diffusion layer, and D the diffusion coefficient. The drug dissolution rate has a direct

proportion to its effective surface area (A) and diffusion coefficient (D), and it could be increased mainly in two ways: decreasing the particle size of the drug and optimizing the wetting characteristics of drug surface (37). All microcrystal improved solubility and increased dissolution rate compared to the pure drug, according to the modified Noyes-Whitney equation. Consequently, smaller particle size provides a larger contact surface with the dissolution medium, accelerating the process of solubilization of the active ingredient being an

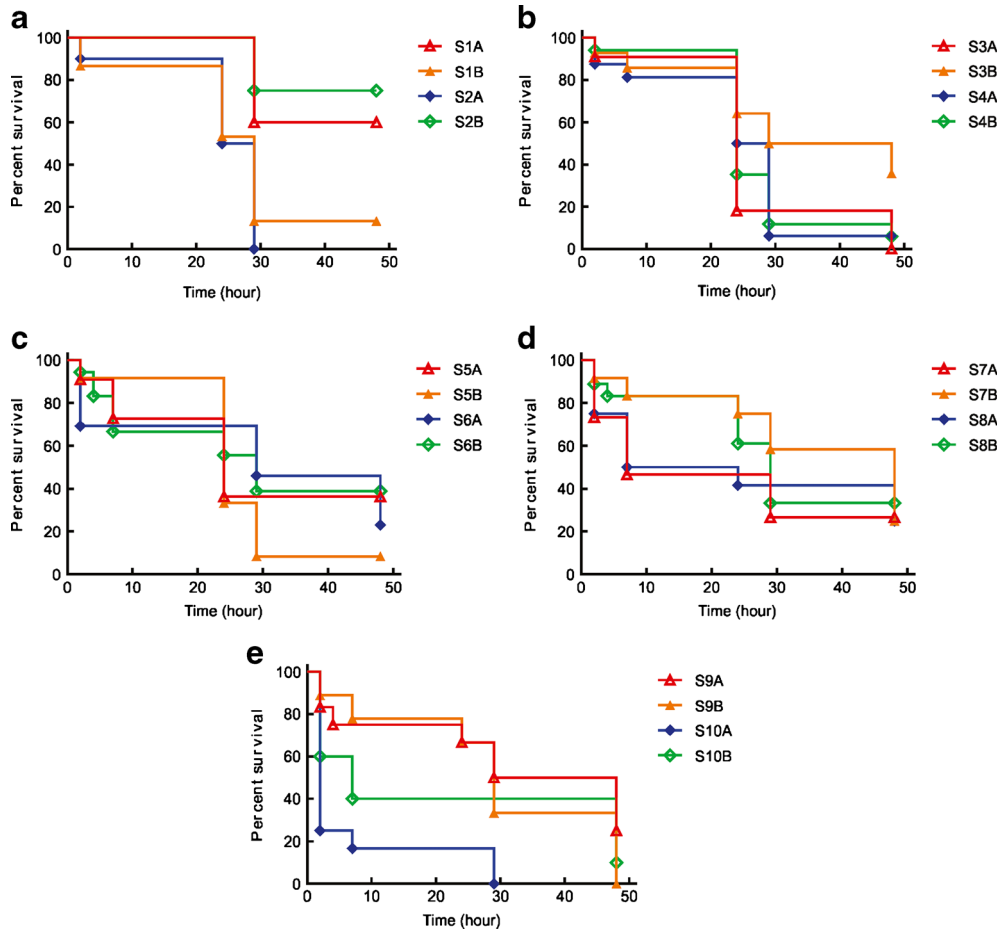


Fig. 6. Survival curves of *T. spiralis* female worms cultured with antiparasitic solutions containing ABZ microcrystal formulations based on various polymers, with and without added surfactant. HPMC hydroxypropylmethylcellulose, HEC hydroxyethylcellulose, CMC carboxymethylcellulose, MC methylcellulose, CH chitosan. Surfactant: poloxamer 338. Survival curves were created with the product limit method of Kaplan and Meier

Table II. Effect of the ABZ Microcrystal Formulations on Survival Parameters of *T. spiralis* Females, After 48 h Incubation

Antiparasitic solution	Variables	
	Median survival (h)	Survival proportion after 48 h (%)
ABZ	Undefined	72.7
S1A ^a	Undefined	60.0
S1B ^b	29	13.3
S2A ^b	26.5	0
S2B ^a	Undefined	75.0
S3A ^a	24	0
S3B ^b	38.5	35.7
S4A ^{a, b}	26.5	6.3
S4B ^a	24	5.9
S5A ^a	24	36.4
S5B ^a	24	8.3
S6A ^a	29	23.1
S6B ^a	29	38.9
S7A ^a	7	26.7
S7B ^a	48	25.0
S8A ^a	15.5	25.0
S8B ^a	29	33.3
S9A ^a	38.5	25.0
S9B ^a	29	0
S10A ^b	2	0
S10B ^a	7	10.0

Differences among formulations were analyzed with the log-rank test. Groups not sharing the same superscript in a row differ significantly ($P < 0.01$), within formulations using the same polymer
ABZ albendazole

effective approach to enhance the dissolution rate and the bioavailability of poorly soluble drugs (8–10).

The size of HPMC, CMC, and MC systems was governed by the polymer concentration. Otherwise, HEC and CH-ABZ microcrystals presented similar particle sizes associated with neither the polymer nor the procedure. By the way, it is significant to mention that analyzing Table I and Fig. 4 for each group of polymers, the Q_{30} values were related with the particle size, being higher values for smaller sizes.

The bottom-up methodology used in these experiments resulted in HPMC systems generating larger ABZ microcrystals than the rest of the formulations. As expected, this finding is

consistent with the results of the dissolution assay as microcrystals formulated with CH showed a better dissolution profile than those containing HPMC. However, ABZ solubility was highest in HPMC microcrystals and lowest in CH microcrystals, an unexpected outcome opposite to that observed in Q_{30} and AUC. The differential responses of the variables analyzed could be due to the characteristics of each polymer, affecting the behavior in the same dissolution medium.

The diffraction patterns of ABZ in the microcrystals were similar to those of the pure drug, indicating that the crystallinity of ABZ did not essentially change. The smaller intensity of some of the peaks of ABZ could be due to the dilution effect in the presence of CH and HEC. Similar results were obtained after analyzing the DSC studies, suggesting that the drug solid structure was not ruled by the presence of the polymers and the surfactant or the manufacturing procedure. The permanence of the crystalline state of ABZ microcrystals could be ascribed to the formulations stability.

The EE obtained results also demonstrated the capability of the bottom-up procedure to achieve microcrystal formulations, avoiding the drug wasting during the production process and, at the same time, recovering almost all of the initial amount of the original drug.

Also yield values for the 20 novel systems indicated that lower polymer concentration optimized the procedure to obtain better batches of microcrystals and the presence of P338 improved yield values. It is worth of mention that apparently the presence of the surfactant enhanced the yield by decreasing the adherence to the spray dryer.

The suitability of five polymers, cellulose derivatives HPMC, HEC, MC, and CMC, and CH was evaluated in an *in vitro* assay. The survival curves in the *in vitro* studies showed that exposure to

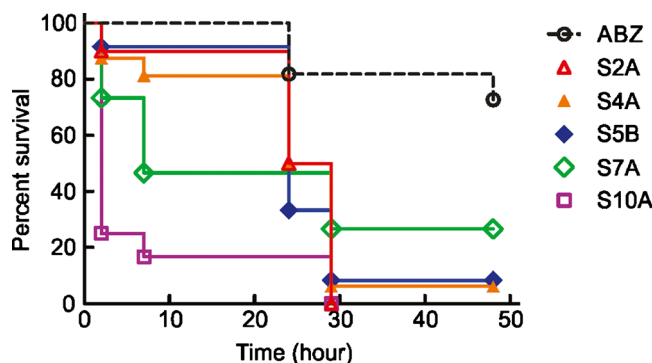


Fig. 7. Survival curves of *T. spiralis* female worms cultured with antiparasitic solutions. Comparison of the *in vitro* anthelmintic effect of the ABZ pure drug solution and the best ABZ microcrystal solutions, on the parasite. Differences between curves were analyzed with the log-rank test (Mantle-Cox test)

Albendazole Microcrystal Formulations

the formulations affected the viability of the adult forms of the parasite in a time and polymer-dependent manner; addition of the surfactant, P338 had little or no impact on improving ABZ effectiveness. In general, low killing efficiencies were associated with high median survival times, as observed in MC-based microcrystals that showed a modest effect on survival of the parasite. On the other hand, at the end of the observation period, elimination of the parasite was complete or nearly complete for HPMC-based S1A and S2A microcrystals, HEC formulations S3A, S4A, and S4B, S5B CMC microcrystals, and CH S9B, S10A, and S10B.

Though, it is currently accepted that small particle sizes have a direct impact on the dissolution rate and bioavailability of poorly soluble drugs. The excellent performance of S10A microcrystals in the *in vitro* assay could contribute to the improvement of ABZ oral formulations.

One of the benefits of an improved performance of a formulation is the possibility of using lower *in vivo* doses of the active ingredient that would be less toxic for the host and would allow longer treatments (38).

The results of the present study indicate that the effective concentration of the ABZ is important to increase parasite mortality and could provide the basis to establish an effective, low-dose therapy for the treatment of trichinellosis. *In vivo* studies are also required to relate the *in vitro* data to the concentrations of the drug clinically effective.

CONCLUSIONS

In summary, all ABZ microcrystal systems improved the solubility and increased the dissolution rate compared to the pure drug. HPMC systems generated large microcrystals while CH-based microcrystals were the smallest. The three-factor analysis indicated that the microcrystals made with HEC or CH appear to be the best options to optimize oral absorption of the API. The *in vitro* evaluation of anthelmintic activity on adult forms of *T. spiralis* identified system S10A as the most effective system for testing therapeutic efficacy *in vivo*.

ACKNOWLEDGMENTS

J.P. is grateful to CONICET (Consejo Nacional de Investigaciones Científicas y Técnicas) for a doctoral fellowship. A.V.C is grateful to CIUNR (Consejo de Investigaciones, Universidad Nacional de Rosario) for a research fellowship.

This work was supported by the Universidad Nacional de Rosario, Consejo Nacional de Investigaciones Científicas y Técnicas (Project N° PIP 112-201001-00194) and Agencia Nacional de Promoción Científica y Tecnológica (Project N° PICT 2006-1126).

REFERENCES

1. Kostewicz ES, Abrahamsson B, Brewster M, Brouwers J, Butler J, Carlet S, *et al.* In vitro models for the prediction of in vivo performance of oral dosage forms. *Eur J Pharm Sci.* 2014;57:342–66.
2. Sosnik A, Augustine R. Challenges in oral drug delivery of antiretrovirals and the innovative strategies to overcome them. *Adv Drug Deliv Rev.* 2016;103:105–20.
3. Gao P, Shi Y. Characterization of supersaturatable formulations for improved absorption of poorly soluble drugs. *AAPS J.* 2012;14(4):703–13.
4. Carrier RL, Miller LA, Ahmed I. The utility of cyclodextrins for enhancing oral bioavailability. *J Control Release.* 2007;123(2):78–99.
5. Leuner C, Dressman J. Improving drug solubility for oral delivery using solid dispersions. *Eur J Pharm Biopharm.* 2000;50(1):47–60.
6. Dahan A, Miller JM, Hoffman A, Amidon GE, Amidon GL. The solubility–permeability interplay in using cyclodextrins as pharmaceutical solubilizers: mechanistic modeling and application to progesterone. *J Pharm Sci.* 2010;99(6):2739–49.
7. Kesisoglou F, Panmai S, Wu Y. Nanosizing—oral formulation development and biopharmaceutical evaluation. *Adv Drug Deliv Rev.* 2007;59(7):631–44.
8. Salazar J, Ghanem A, Müller RH, Möschwitzer JP. Nanocrystals: comparison of the size reduction effectiveness of a novel combinative method with conventional top-down approaches. *Eur J Pharm Biopharm.* 2012;81(1):82–90.
9. Kakran M, Shegokar R, Sahoo NG, Al Shaal L, Li L, Müller RH. Fabrication of quercetin nanocrystals: comparison of different methods. *Eur J Pharm Biopharm.* 2012;80(1):113–21.
10. Kawabata Y, Wada K, Nakatani M, Yamada S, Onoue S. Formulation design for poorly water-soluble drugs based on biopharmaceutics classification system: basic approaches and practical applications. *Int J Pharm.* 2011;420(1):1–10.
11. Yang L, Chu D, Wang L, Ge G, Sun H. Facile synthesis of porous flower-like SrCO₃ nanostructures by integrating bottom-up and top-down routes. *Mater Lett.* 2016;167:4–8.
12. Sinha B, Müller RH, Möschwitzer JP. Bottom-up approaches for preparing drug nanocrystals: formulations and factors affecting particle size. *Int J Pharm.* 2013;453(1):126–41.
13. Hu X, Chen X, Zhang L, Lin X, Zhang Y, Tang X, *et al.* A combined bottom-up/top-down approach to prepare a sterile injectable nanosuspension. *Int J Pharm.* 2014;472(1–2):130–9.
14. Paredes AJ, Llabot JM, Sánchez Bruni S, Allemandi D, Palma SD. Self-dispersible nanocrystals of albendazole produced by high pressure homogenization and spray-drying. *Drug Dev Ind Pharm.* 2016;42(10):1564–70.
15. Yallapu MM, Nagesh PKB, Jaggi M, Chauhan SC. Therapeutic applications of curcumin nanoformulations. *AAPS J.* 2015;17(6):1341–56.
16. de Waard H, Frijlink HW, Hinrichs WLJ. Bottom-up preparation techniques for nanocrystals of lipophilic drugs. *Pharm Res.* 2011;28(5):1220–3.
17. Zhang Y, Hu X, Liu X, Dandan Y, Di D, Yin T, *et al.* Dry state microcrystals stabilized by an HPMC film to improve the bioavailability of andrographolide. *Int J Pharm.* 2015;493(1–2):214–23.
18. Tu L, Yi Y, Wu W, Hu F, Hu K, Feng J. Effects of particle size on the pharmacokinetics of puerarin nanocrystals and microcrystals after oral administration to rat. *Int J Pharm.* 2013;458(1):135–40.
19. Elsayed A, Al-Remawi M, Qinna N, Farouk A, Al-Sou'od KA, Badwan AA. Chitosan–sodium lauryl sulfate nanoparticles as a carrier system for the in vivo delivery of oral insulin. *AAPS PharmSciTech.* 2011;12(3):958–64.
20. Cervera MF, Heinämäki J, de la Paz N, López O, Maunu SL, Virtanen T, *et al.* Effects of spray drying on physicochemical properties of chitosan acid salts. *AAPS PharmSciTech.* 2011;12(2):637–49.
21. Sezer AD, Hatipoglu F, Cevher E, Oğurtan Z, Bas AL, Akbuğa J. Chitosan film containing fucoidan as a wound dressing for dermal burn healing: preparation and in vitro/in vivo evaluation. *AAPS PharmSciTech.* 2007;8(2):94–101.
22. Higuera L, López-Carballo G, Cerisuelo JP, Gavara R, Hernández-Muñoz P. Preparation and characterization of chitosan/HP-β-cyclodextrins composites with high sorption capacity for carvacrol. *Carbohydr Polym.* 2013;97(2):262–8.

23. Amin M, Abbas NS, Hussain MA, Edgar KJ, Tahir MN, Tremel W, *et al.* Cellulose ether derivatives: a new platform for prodrug formation of fluoroquinolone antibiotics. *Cellulose*. 2015;22(3):2011–22.
24. Regdon G, Hegyesi D, Pintye-Hódi K. Thermal study of ethyl cellulose coating films used for modified release (MR) dosage forms. *J Therm Anal Calorim*. 2012;108(1):347–52.
25. Baltzley S, Mohammad A, Malkawi AH, Al-Ghananeem AM. Intranasal drug delivery of olanzapine-loaded chitosan nanoparticles. *AAPS PharmSciTech*. 2014;15(6):1598–602.
26. Charoenthai N, Kleinebudde P, Puttipipatkachorn S. Influence of chitosan type on the properties of extruded pellets with low amount of microcrystalline cellulose. *AAPS PharmSciTech*. 2007;8(3):99–109.
27. Dubey RR, Parikh RH. Two-stage optimization process for formulation of chitosan microspheres. *AAPS PharmSciTech*. 2009;5(1):20–8.
28. Piyakulawat P, Praphairaksit N, Chantarasiri N, Muangsin N. Preparation and evaluation of chitosan/carrageenan beads for controlled release of sodium diclofenac. *AAPS PharmSciTech*. 2007;8(4):120–30.
29. Wang Y, Li P, Kong L. Chitosan-modified PLGA nanoparticles with versatile surface for improved drug delivery. *AAPS PharmSciTech*. 2013;14(2):585–92.
30. Dayan AD. Albendazole, mebendazole and praziquantel. Review of non-clinical toxicity and pharmacokinetics. *Acta Trop*. 2003;86(2–3):141–59.
31. Daniel-Mwambete K, Torrado S, Cuesta-Bandera C, Ponce-Gordo F, Torrado JJ. The effect of solubilization on the oral bioavailability of three benzimidazole carbamate drugs. *Int J Pharm*. 2004;272(1–2):29–36.
32. United States Pharmacopeia, USP. United States pharmacopeia and national formulary convention. Rockville (MD); 2009.
33. Khan KA. The concept of dissolution efficiency. *J Pharm Pharmacol*. 1975;27(1):48–9.
34. García A, Leonardi D, Piccirilli GN, Mamprin ME, Olivieri AC, Lamas MC. Spray drying formulation of albendazole microspheres by experimental design. In vitro–in vivo studies. *Drug Dev Ind Pharm*. 2015;41(2):244–52.
35. Dražić S, Sladoje N, Lindblad J. Estimation of Feret's diameter from pixel coverage representation of a shape. *Pattern Recogn Lett*. 2016;80:37–45.
36. Vasconi MD, Bertorini G, Codina AV, Indelman P, Masso RJD, Hinrichsen LI. Phenotypic characterization of the response to infection with *Trichinella spiralis* in genetically defined mouse lines of the CBI-IGE stock. *Open J Vet Med*. 2015;5(5):12.
37. Bikiaris DN. Solid dispersions, part I: recent evolutions and future opportunities in manufacturing methods for dissolution rate enhancement of poorly water-soluble drugs. *Expert Opin Drug Deliv*. 2011;8(11):1501–19.
38. Codina AV, García A, Leonardi D, Vasconi MD, Di Masso RJ, Lamas MC, *et al.* Efficacy of albendazole:β-cyclodextrin citrate in the parenteral stage of *Trichinella spiralis* infection. *Int J Biol Macromol*. 2015;77:203–6.